Appl. Phys. B 61, 101–110 (1995)

Applied Physics B Lasers and Optics

Investigation of collisionally induced stimulated scattering in sodium vapor with temporal and spectral resolution

Z. Konefal, M. Ignaciuk

Institute of Experimental Physics, University of Gdańsk, ul. Wita Stwosza 57, PL-Gdańsk 80-952, Poland
(E-mail: FIZZK@halina.univ.gda.pl.)

Received: 11 July 1994/Accepted: 7 August 1994

Abstract. In this work we present fully time-resolved spectra of Amplified Spontaneous Emission (ASE) and Stimulated Raman Scattering (SRS) in sodium vapor. We observe that the ASE signal precedes the SRS emission, and the peak of the amplified Stokes pulse is delayed with respect to the peak of the laser pulse. The time evolution of the line widths of the ASE and Raman signals is also shown. We find that the line widths of the stimulated fluorescence component (ASE) and the stimulated Raman radiation change with time. Both spectra start as small narrow fluctuating lines, then the line widths reach maximum values and thereafter decrease with time.

PACS: 32.80.Wr; 32.90.+a

Recently, there has been some interest in studying atom-field interaction dynamics in the framework of time-dependent spectra and also a great deal of effort has been put towards demonstrating that the dynamics of atomic collisions can be modified by the presence of intense laser fields.

A lot of theoretical work has been reported but the time-dependent spectra were measured only in relatively few experiments. Golub and Mossberg [1] measured the transient spectra of strong-field resonance fluorescence. Shevy and Rosenbluh [2] did not fully present the time-resolved behavior of the emission of parametric four-wave mixing and stimulated three-photon scattering, but they rather gave the qualitative time evolution of the processes. In this work we present the fully time-resolved dependence of the Amplified Spontaneous Emission (ASE) and Stimulated Raman Scattering (SRS) spectra in sodium vapor. During the near-resonant excitation of the $P_{3/2}$ excited state of sodium by a laser beam, collisionally induced ASE and SRS were observed [3]. The production of ASE due to the $3^2P_{1/2}$–$3^2S_{1/2}$ transition (the D_1 line) and SRS connected with the $3^2P_{3/2}$, $3^2P_{1/2}$ levels in sodium vapor mixed with helium was described theoretically by Czub et al. [4] and measured recently by Konefal and Ignaciuk [5]. These effects were also investigated by Dabagyan et al. in a mixture of potassium vapor with helium [6, 7].

The radiation field interacting with a three-level system is essential in many problems of quantum optics, e. g., pulse propagation (including solitons), stimulated Raman scattering, superfluorescence, and parametric amplification. In the usual theoretical treatment of Raman scattering, the pump laser is assumed to be tuned to a far-off resonance from any higher intermediate state which provides the dipole coupling that allows Raman scattering. Distinct Raman and fluorescence components occurring simultaneously on the same transition were observed in experiments. Wynne and Sorokin [9] noted separate spectral components and their competition, when tuned near a resonance line in potassium vapor. Raymer and Carlsten [10] observed the simultaneous amplification of both Raman and fluorescence light in experiments on atomic thallium in argon buffer gas.

The study of SRS allows a better understanding of some issues that are involved in the distinction between ASE and superfluorescence. One can say that when the dephasing rate is sufficiently high to overcome the tendency of the atoms to emit coherently, then the emission is incoherent and ASE-like. Otherwise, it is coherent and superfluorescence-like. From the quantum-optics theoretical point of view the SRS problem is interesting because of the necessity to treat it in a time-dependent manner, including spatial propagation in the presence of spontaneous quantum noise and collisional dephasing noise. The quantum theory of stimulated Raman scattering which takes into account three-dimensional propagation and collision dephasing allowing the study of the spatial and temporal coherence properties of generated Stokes light, was developed by Raymer et al. [11]. Swanson et al. [12] showed that as little as one input Stokes photon per temporal mode can influence the phase of a Raman amplifier, providing convincing evidence that a Raman amplifier can indeed be operated close to the quantum limit. A few initial scattering photons which

seed the stimulated gain process giving rise to the well-collimated beam with a relatively narrow bandwidth, a high degree of spatial coherence, with a well-defined phase, amplitude, and temporal structure on any given shot. However, since the process is initiated by random zero-point motions of the field, the fluctuations of the phase of the field were observed to be uniformly and randomly distributed from shot to shot.

1 Theoretical considerations

1.1 Population redistribution in NaHe *system*

Let us consider three-level atoms with energy levels $E_1 < E_2 < E_3$ in the field of laser radiation that is quasi-resonant with the $1 \rightarrow 3$ transition. Transitions $1 \rightarrow 3$ and $1 \rightarrow 2$ shown in Fig. 1. are allowed in the dipole approximation. The collisions with buffer atoms make transition between levels 2 and 3 possible. When the laser frequency (ν_L) is detuned from the $3S_{1/2} \rightarrow 3^2P_{3/2}$ resonance, two different physical processes can occur: amplified spontaneous emission (ν_{ASE}) and excited-state Raman scattering (ν_{SRS}). In the experiments, the excited state $3P_{3/2}$ is first populated by the laser pulse and the collisions with buffer gas result in the population of the $3P_{1/2}$ state, from which stimulated ASE and SRS scattering next occur. These events are displaced against each other in time. For the case of resonant pumping these two contributions to fluorescence cannot be separately identified. For off-resonant pumping, however, the two processes are spectrally distinguishable because of the difference in the frequencies of scattered photons. It should be mentioned that the terminating virtual state for Raman scattering is placed near the $S_{1/2}$ state (Fig. 1). It means that this state is a dominant intermediate state for the process mentioned above [8].

The relationship which theoretically explains the population inversion between the $3^2P_{1/2}$ and $3^2S^{1/2}$ levels, which is important for Raman generation, follows from the detailed balance principle and is expressed by

$$\gamma_{23} = 2\gamma_{23}\exp\left(\frac{-(E_3 - E_2)}{kT}\right), \tag{1}$$

where γ_{32} is the collisional transfer rate from $P_{3/2}$ to $P_{1/2}$, while γ_{23} corresponds to the opposite process. As demonstrated in [4], in the pressure and laser intensity ranges corresponding to the experiment the populations of $3P_{1/2}$ and $3S_{1/2}$ are very close to the half-population of the $3P_{3/2}$ level. The inversion occurs when [13]

$$2\gamma_{32} \geq \gamma_{23} + \gamma_1, \tag{2}$$

where γ_1 is the radiative damping constant. It is very easy to show, using the data presented in [13], that (2) is satisfied for all buffer gas pressures which were used in our experiment. As mentioned above, the ASE and SRS effects are caused by the effective population of the $3^2P_{1/2}$ level, resulting from collisions of the excited sodium

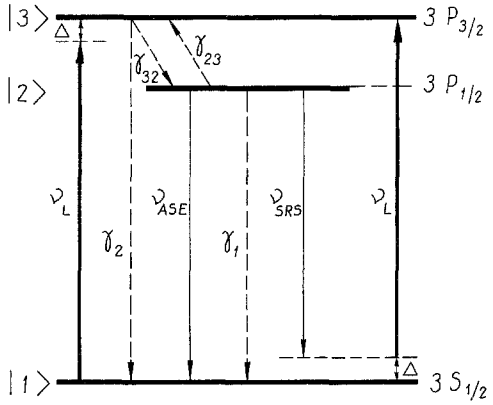

Fig. 1. First three energy levels of sodium, with the driving laser at frequency (ν_L, tuned near the D_2 transition. The collision-induced fluorescence at ν_{ASE}. Electron Raman scattering at the Stokes frequency ν_{SRS}. The collision transfer of population is shown as *broken lines*

atoms with buffer gas atoms during the laser pulse. When taking into account that for atmospheric pressure of He, γ_{32} for the NaHe mixture is of the order of $10^{10}\ s^{-1}$ it is evident that this transfer of population is highly effective.

The inversion between the ground and first excited level can be achieved only when strong absorption of laser light takes place. One can easily show [14] that the absorption in the region of the principle resonance line (e. g., the D_2 line) will be strong over a wider range of detuning of the laser pump.

1.2 Saturation

Additionally, at high intensities of the laser pump (I_p), the density n_1 of the lower state can noticeably decrease while the upper state density n_3 increases as mentioned above. In this case the saturation process should be included in our considerations. I_{sat} may be written in terms of the absorption cross-section and the decay time T_1 of the upper level of the transition. For a pulse shorter than T_1 (in our case $T_1 = 1.6 \times 10^{-8}$ ns, the laser pulse about 8 ns), the saturation is characterized by a saturation energy flux (energy/area), $E_{sat}/A = I_{sat} \cdot T_1 = \hbar\omega/2\sigma$ [18]. In the case considered the estimated value for resonance excitation is of the order of $3 \times 10^{-13}\ cm^2$, and therefore the corresponding saturation energy flux is $\approx 2.4 \times 10^{-3}\ J/m^2$. This value is estimated for resonance excitation, and it will increase as the square of the detuning from the resonance. The experimental values of the saturation energy densities are even five or six times greater than those calculated [14].

Taking into account our measurements of the dependence of ASE and SRS energies on the excitation intensity [5] (Fig. 5), it can be noted that the saturation starts from the laser intensity of 7 kW. In this experiment, the laser beam was focused on the input face of the cell to a diameter of about 1 mm, giving an experimental value of $1.8 \times 10^{-2}\ J/cm^2$ for an 8 ns laser pulse. This is the low limit value, since inside the cell the diameter of the waist

of the beam can be narrowed. The rigorous treatment of atom saturation requires a dynamic approach. In our theoretical estimations we take into account only the single-photon absorption saturation parameter, whereas in practice atom depletion is also present. In this experiment the atoms can be recirculated many times during the pumping pulse. The ASE process brings the atoms from the $3P_{1/2}$ level very fast back to the ground state, and the atoms are again available for the pump pulse. The SRS process takes the atoms away also from the $3P_{1/2}$ level but, as seen in Fig. 1, it leaves them in the $3P_{3/2}$ state. From this state the atoms are also very fast transported by collisions ($\gamma_{32} \approx 10^{10}$) to $3P_{1/2}$ and participate again in the generation of SRS or ASE signals. Such a rapid recirculation of atoms prevents saturation in the system.

1.3 Small-signal gain

Weak spontaneous emission can be treated as an injected Stokes signal. Following the approach described by Dreyfus and Hodgson [20] only Stokes light emitted into a solid angle passing out the end of the pumped region experiences the maximum gain. An additional simplification follows from the observation that the gain should be large enough so that only photons emitted spontaneously near the entrance to the cell are important. The spontaneous starting level can be calculated by the use of the ordinary Raman scattering cross-section for Na [8]. For very small ratios of the injected Stokes I_s(in)-to pump intensity (I_0), the relation for the gain G in the amplifier can be written in the form $I_s(\text{out})/I_s(\text{in}) = \exp(Gz)$, where z is the propagation distance [19]. The energy conversion efficiency in our systems for generating ASE or SRS is known to be of the order of 1% [3]. Hence, $I_s(\text{out}) = 0.01 \cdot I_0$ and therefore $GL = \ln(0.01 \cdot I_0/I_s(\text{in}))$. The value calculated from the latter equation for Gz is 26. The I_s(in) was calculated according to the procedure given in [19]. It should be mentioned that taking the standard value for the residual quantum noise at a Stokes frequency of $I_s(0) = 10^{-4}\,\text{W/cm}^2$, a threshold gain equal to 25 can be obtained [21]. Such a theoretical simplified model based on the notion that the output is only due to amplified spontaneous Raman scattering yields, in fact, a gain value much higher than that observed. It should be mentioned that the small-signal gain was estimated in [3] for ASE to be equal to 22.

1.4 Spectral characteristics of one- and two-photon pulse amplifiers

In general, the spectral line of the ASE signal in a single quantum amplifier is a combination in a certain proportion, of Gaussian and Lorentzian line shapes. For homogeneous broadening, which is important in the case considered, when we deal with high buffer gas pressure and no saturation, the gain is Lorentzian. The spectral width can be simply written in the form [22]

$$\Delta\nu_{\text{hom}} = \Delta\nu_{\text{h}} \sqrt{\frac{\ln 2}{g(0)_{\text{hom}} z}}. \tag{3}$$

Thus, the narrowing effect becomes important when the product $g_f(0)_{\text{hom}} \cdot z$ is greater than unity. For an unsaturated inhomogeneously broadened amplifier, a similar narrowing effect takes place.

When the intensity of the amplified spontaneous emission reaches the saturation level, the behavior of the spectrum becomes considerably more complex. Generally speaking, in a homogeneously broadened amplifier the saturation slows the narrowing process down, while in an inhomogeneously broadened amplifier it restores the line to its original inhomogeneous shape [22].

The spontaneous or low-gain Raman scattering has a spectral width given by the sum of the Raman line width, Γ(HWHM), and the laser bandwidth Γ_L. When the laser bandwidth is much smaller than the Raman line width, the spontaneous scattering has a Lorentzian half-width of Γ. When the gain becomes high ($Gz > 1$), the gain narrowing distorts the Lorentzian line shape by amplifying the central part of the Stokes line more strongly than the line wings. The SRS has the same spectrum as the laser when the spectrum of the latter is broader than that of the scattering line. For steady-state high-gain Stokes intensity $I_s(z, \infty)$, the Stokes spectrum is found to be [23]

$$P_s(\omega) = I_s(z, \infty)\left(\frac{Gz}{\pi\Gamma^2}\right)\exp\left(-\frac{Gz}{\Gamma^2}\omega^2\right). \tag{4}$$

This equation describes a gain-narrowed line profile. The spectrum becomes Gaussian with a gain-narrowed line width of about $\Gamma/(Gz)_{1/2}$.

Experimental measurements of Stokes line widths have revealed a very considerable broadening, with line widths up to two orders of magnitude greater than the Doppler width of the Raman transition.

1.5 Dephasing time

For an undriven atom, the dipole moment decays to zero in the characteristic time T_2, which is known as the dipole dephasing time. The dephasing time of Raman scattering medium is defined as the inverse of the Raman scattering bandwidth $T_2 = 1/\pi\Delta\nu_r$. In order to determine T_2 one should take the value of $\Delta\nu_r$ equal to the line width of the Stokes signal ($2\Gamma = \Delta\nu_r$). It is known that there is a discrepancy between the theoretical and experimental values of the Stokes line width [14]. However, the SRS experiments with potassium and cesium show that by taking values of Γ equal to the observed line widths of the Stokes output it is possible to obtain a reasonable agreement between the measured and calculated values of the threshold and tuning range [14]. We simply assume that this empirical procedure is fulfilled also in our case. The last equation implies that for the observed line width of the order of $1\,\text{cm}^{-1}$, the response time T_2 is about 0.1 ns.

1.6 Temporal and spatial properties of stimulated processes

The three-dimensional nature of the propagation can lead to the interference of the light, in different spatial modes, resulting in the formation of a speckle pattern on the generated Stokes beam. The spontaneous scattering excites many radiation modes with random phases, whereas the propagation through the pencil-shaped pumped volume filters the light spatially and amplifies only modes within some small solid angle. For larger solid angles, several or many modes are amplified and propagate out of the end of the medium, giving rise to an interference or speckle pattern. The spatial properties of the stimulated signal depend on the Fresnel number $F = A/\lambda_s \cdot L$, where A and L are the cross-sectional area and length of the pumped volume and λ_s is the Stokes wavelength. When F is close to unity, the field is assumed to be in a single spatial mode. As F increases, more and more spatial modes are excited. When the collisional dephasing rate Γ is sufficiently small to have no effect during the Stokes pulse, the scattering is said to be in the transient regime. This is true when the laser pulse duration τ_L satisfies $\tau_L \Gamma < GL$. This arises from the requirement that dephasing can be negligible for the duration of the Stokes pulse. This is not the case in our experiment.

We should take into account that in the Stokes signal we can have more then one temporal mode. Temporal fluctuation of Stokes intensity results from the interference between different temporal modes. When F and $\tau_L \Gamma/GL$ are small (≤ 1), a single spatial-temporal mode is dominant in the Stokes emission. When $F = 1$ and $\tau_L \Gamma/GL$ is large, a single spatial mode is present and many temporal mode are excited, i. e., the pulse is not temporally coherent. Such events should be observed in our experiments. The ratio $\Gamma \tau_L/GL$ is approximately proportional to the number of temporal modes excited. The number of excited spatial modes is proportional to F^2.

2 Experiment

The experimental apparatus is shown in Fig. 2. A grazing incidence-type dye laser, pumped by a N_2 laser, was used to give 8 ns pulses with a peak power up to 15 kW and a line width of 0.1 cm^{-1}. This laser is described in detail elsewhere [5]. Instead of one-stage amplification, two-stage amplification was used. The experiment consisted in irradiating a 12 cm column of sodium vapor contained in a pyrex cell working in the heat-pipe regime. Noble gases were admitted to the cell at pressures in the range of 25 to 100 kPa.

Mirrors and beam-splitters were installed in the set-up to investigate the stimulated emission after one (SP) or two passes (DP) of the pump laser and of ASE and SRS beams through the cell. The radiation leaving the cell was focused on the entrance slit of the spectrograph. Instead of a photographic plate, the spectrograph was equipped with commercially available macrophotography lens allowing magnifications of the output spectra. A beam splitter divided the magnified beam into two light paths. A movable slit driven by a stepping motor was placed on one of the paths. The light signal in this path was registered with a fast (1.2 ns rise time) photomultiplier. Using the signal divider the lines from the sodium lamp (position markers) and pulse signals (ASE, SRS, laser) averaged by a boxcar gate could be measured simultaneously (using a voltmeter). The boxcar 220 ps gate was moved in 0.5 ns steps by a computer via a voltage source. At each frequency step, the boxcar gate moved in time and in each position the signals are accumulated.

The pulse energy of each laser shot was measured, and the signal was stored in the computer memory only if the pulse energy was within a small percentage of a preset value. The resolution is an important issue in the experiment. The narrowest laser line observed was 0.01 cm^{-1}. The spectral width of almost all the features reported was not instrumentally limited. In the second path the signals were detected by a linear photodiode array. The instrument was designed to observe spectrally and temporally resolved stimulated emission from the cell.

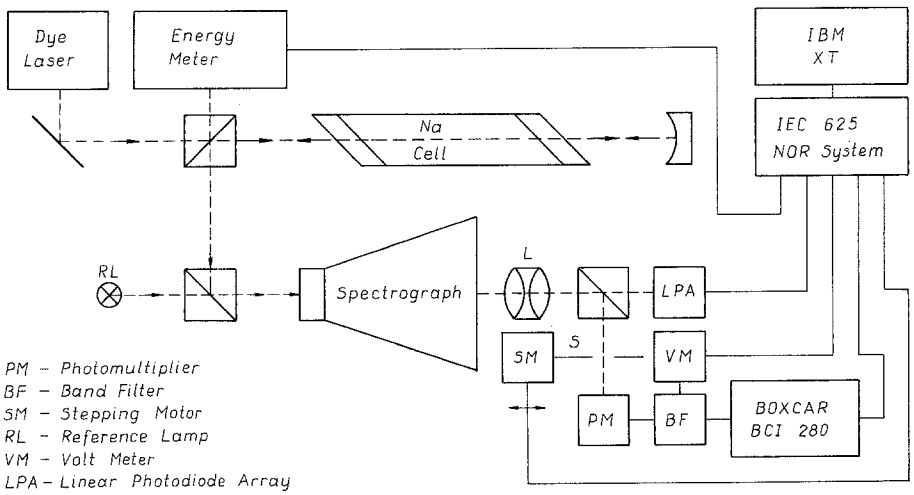

Fig. 2. Schematic of the experimental apparatus

3 Results and discussion

In the experiment, we measured the temporal and spectral evolution of the ASE and SRS signals as a function of intensity and frequency of the exciting radiation, and of the buffer gas and sodium vapor pressures.

Figures 3 and 4 show the temporal evolution of the spectra. Three well-resolved peaks can be distinguished: the pump laser line on the left, the ASE line in the center and the SRS line on the right. The pump laser, ASE, and SRS signals were obtained in a sequence of slit scans. A slightly different time (0.5 ns scan) was chosen for each scan. Laser detuning was 3 cm^{-1}, the buffer gas pressures were 89.0 kPa and 76.6 kPa, respectively. We found that the ASE and SRS signals were present only during the laser pulse. Generally, the ASE and SRS signals are delayed with respect to the pump pulse. This fact reflects the time-dependent collisional transfer of population to the upper $3P_{1/2}$ state. From these spectra it can be seen that the ASE signal appears first. In course of time, the SRS signal begins to grow. The SRS signal lasted approximately 0.5 ns longer than the ASE one, which was no longer detectable. The initial growth of both pulses depends on the gain value for those two processes. Because the fluorescence amplification results from a one-photon transition, it will, in general, be amplified quicker than the two-photon Raman process. This type of behavior was confirmed by theoretical calculation carried out by Herman et al. [24].

These two spectra demonstrate also how the buffer gas pressure influences the ASE and SRS signals for this large laser detuning (3 cm^{-1}). As shown above, a rather strong absorption occurs even when the laser is detuned far from resonance, but the collision not only can greatly enhance the excitation by breaking the adiabaticity or shifting the energy levels of the active atom into resonance with the external field, but also recirculate the population between the fine-structure sublevels. Thus, for higher gas pressures, the population of the $3S_{1/2}$ level is very efficiently transferred to the $3P_{1/2}$ level via the $3P_{3/2}$ level, and consequently, the ASE component [5] grows more rapidly with pressure than the Raman component. Additionally, the strong single-photon absorption process takes significant amount of energy away from the pump pulse. Raman scattering is known to result from two photon processes. It means that the Raman component strongly depends on the pump laser intensity.

At lower pressures and large detuning the Raman component can completely dominate the ASE one, so that the latter is never amplified. This is exactly what can be seen in Fig. 4. One should bear in mind that the population of the $3P_{1/2}$–$3S_{1/2}$ levels is inverted only when the relation given by (2) is satisfied. This inversion, as mentioned above, is connected with the ASE signal. In the case of the Raman transition, the inversion between $3P_{1/2}$ and $3S_{1/2}$ levels (which is required for the generation of the SRS signal) is fulfilled even at low buffer pressure, this resulting from (1). This pressure should be high enough that the inversion takes place in time shorter than that of the laser pulse.

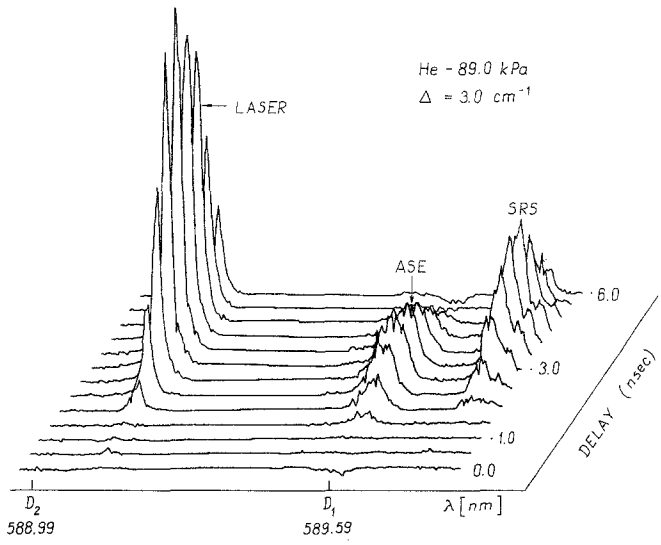

Fig. 3. Three-dimensional plot of the recorded pump laser, ASE and SRS signals consisting of data obtained in sequence of slit scans. A slightly different time (0.5 ns scan) was chosen for each different scan. Helium pressure 89.0 kPa, laser detuning $\Delta = 3$ cm^{-1}

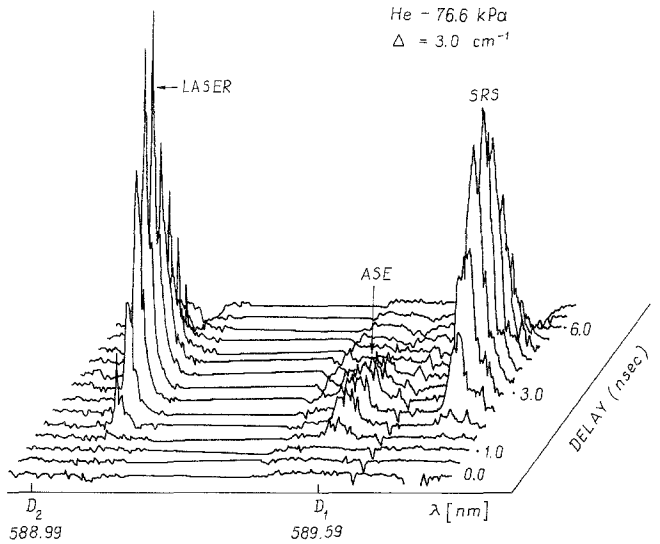

Fig. 4. Time evolution of the spectra obtained by moving the 200 ps wide boxcar gate in 0.5 ns steps. Buffer gas pressure 76.6 kPa, laser detuning $\Delta = 3$ cm^{-1}

A reduction of the duration of the pulse after it had passed the cell was observed. The laser pulse changes its duration from 8 to 3.5 ns. The change in the width is connected with the strong absorption of the leading edge of the pulse. This absorption pushes on the inversion in the system.

Figure 5a shows the temporal evolution of the ASE and SRS signals for two temperatures of the cell (395° C and 422° C). The helium pressure was 77.8 kPa. Figure 5b displays this evolution for a cell temperature of 395° C and for a He pressure of 97.1 kPa. Detuning was 1.4 cm^{-1} and the laser power 15 kW. This dependence was obtained using a single pass cell configuration. Figure 5a shows that for the rather low helium pressure

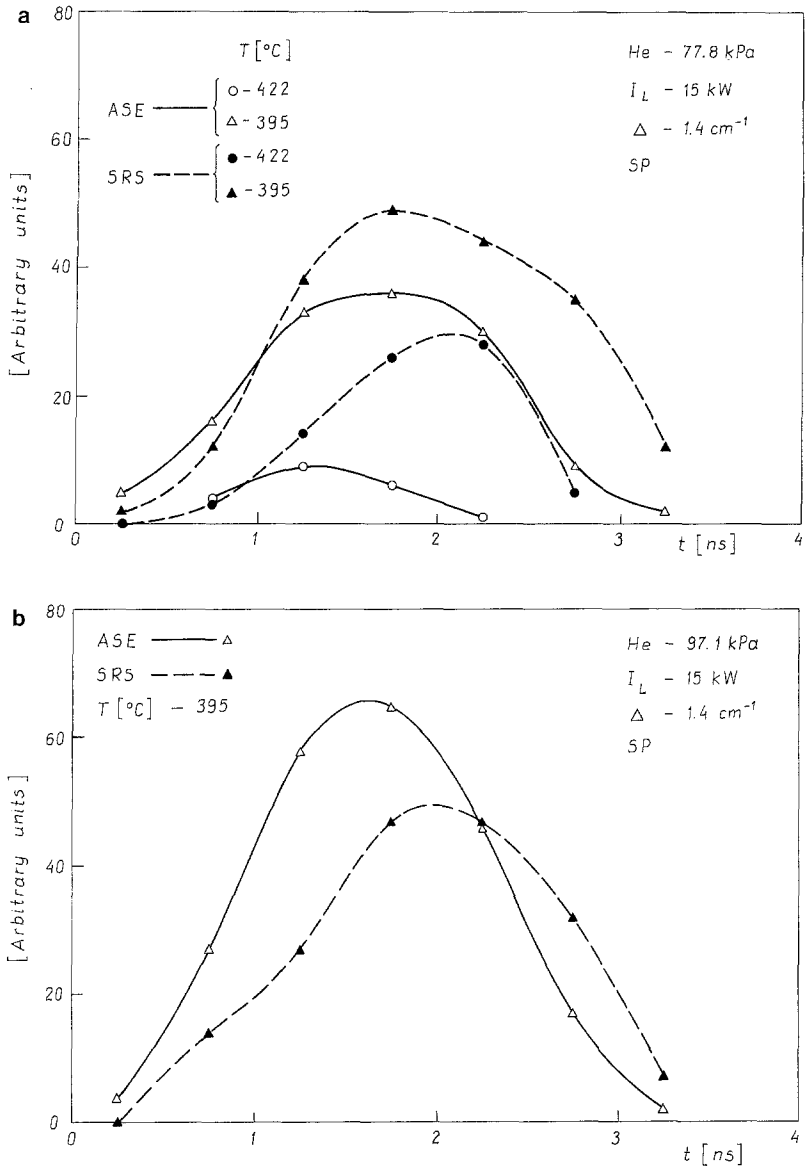

Fig. 5a, b. Time evolution of the ASE and SRS signals. The helium pressure: (**a**) 77.8 kPa, (**b**) 97.1 kPa, laser detuning $\Delta = 1.4\ \mathrm{cm}^{-1}$

(77.8 kPa) the SRS signal is roughly 0.5 ns delayed relative to the ASE signal. Also the intensity of the SRS signal is higher than that of the ASE signal in the middle and end parts of the signals. The intensity ratio of the SRS and ASE signals increases with growing temperature. This effect is connected, on the one hand, with the decrease of the ASE signal and, on the other hand, with the increase of the gain for SRS signal. The decrease of the ASE signal is apparently due to absorption of the ASE photons at the end of the cell where the laser pump is too small to build up the population inversion of $3P_{1/2}$ with respect to the $3S_{1/2}$ state. The ASE signal is resonant with the $3P_{1/2} \rightarrow 3S_{1/2}$ transition, but the Raman light can propagate through a medium which is almost transparent for it, because this signal is not in resonance with any real transition [5]. The delay between the intensity maxima of the ASE and SRS signals also increases when increasing the cell temperature. In this case the duration of the SRS signal is also longer than that of the ASE.

Figure 5b exhibits the temporal behavior of the ASE and SRS emissions for 97.1 kPa buffer gas pressure. The temperature of the cell was 395° C and the laser power was 15 kW. It can be seen that for high buffer gas pressures the time duration of these two signals is nearly the same and the ASE and SRS appear and delay roughly at the same moment. Only the maximum of the SRS intensity is delayed in comparison with the ASE maximum, as in the low pressure case.

Figure 6 depicts the temporal behavior of the ASE and SRS components for large detuning of the pump laser. As can be seen, for large detuning the time duration of ASE (even for high helium pressure) is shorter than that for small detuning. In the case of large detuning and at high cell temperature, the maximum intensity of SRS is almost three times as high as that of ASE. In the latter case, the suppression of the ASE component by the Raman component is considerable even when the buffer-gas pressure in the cell is high. As mentioned above, the intensity of the ASE signal decreases with an increase of the cell temperature if the laser power is too small to build up the population inversion in the whole cell. Additionally, for large detuning of the pump laser, the absorp-

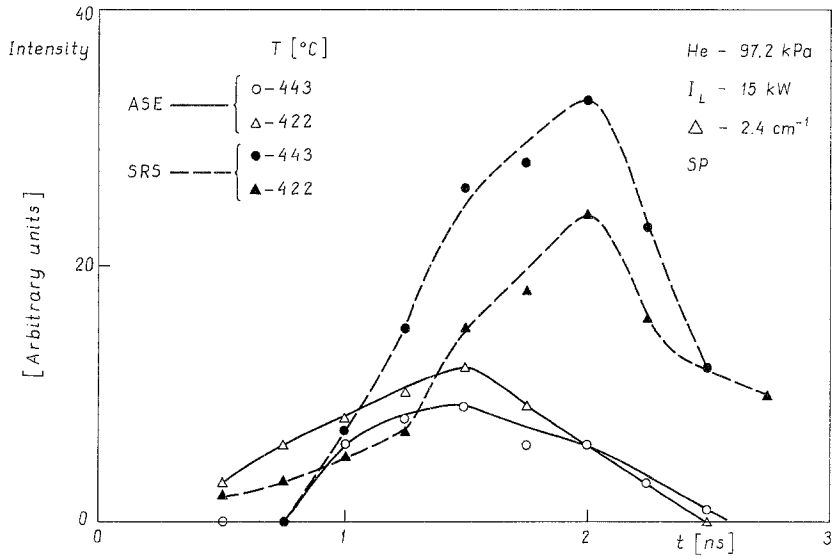

Fig. 6. Temporal behavior of the ASE and SRS components for large detuning of the pump laser ($\Delta = 2.4\ \mathrm{cm}^{-1}$) and a high cell temperature

tion is not as high as in the case of near resonance pumping and then, as already known, the Raman component grows more rapidly than the fluorescence one.

Our experimental set-up allows also measuring line shapes for the SRS and ASE signals. As shown in [25], the shape of the energy spectrum of SRS fluctuates from pulse to pulse. The energy content of each Stokes pulse is expected to be a random quantity due to quantum noise. The initial fluctuation can be amplified to obtain large-scale fluctuations in the energy, spectrum and temporal shape of the output pulse. These temporal fluctuations connected with our experimental set-up did not allow us to see any ringing oscillations of the ASE and SRS components. Such a structure would be washed out in our boxcar averaging system. It should be mentioned that in our experiment the laser beam was strongly focused on the cell, the Fresnel number was less than unity, and a single spatial mode was excited. The temporal fluctuation of the Stokes pulse intensity were studied experimentally by Ramer et al. [26]. They found that the pulse shape varies randomly from pulse to pulse, for an interaction volume with a small Fresnel number. In general, the shape of the Stokes pulse is found by the linear combination of all the temporally coherent modes with random weights. As shown in Sect. 1–6, one should have many temporal modes in the system.

A related observation was also made in the frequency domain. By examining the Stokes pulse-energy spectrum of successive shots, MacPherson et al. [27] observed spectral fluctuations that correspond to a random excitation of temporally coherent modes. It was found that the spectrum of a single Stokes pulse has several peaks, each of which was much narrower then the ensemble-averaged line width. The position and widths of the peaks varied randomly from one Stokes pulse to another although the ensemble-averaged spectrum was in agreement with the gain-narrowed spectrum predicted by the theory.

As mentioned above, the first spontaneously scattered Stokes photons, which travel in the proper direction, can serve as a source of such fluctuations in the strong amplification case. One should also take into account that the conventional dye laser carries, with some background emission, a spectral distribution centered around the maximum of the tuning range. The dye laser background usually shows the mode structure of the cavity. Such photons can serve as input photons of one-pass amplifier. The output signal should have a similar periodic structure. Such a dye-dependence of some emissions generated by the axially phase-matched parametric six-wave mixing processes was reported in [28].

If the amplifications take place in the linear regime, where neither laser field nor atomic population are depleted, the statistical properties of the initiating photons are preserved. But if the amplification takes place in the nonlinear regime, than it is expected that the statistical properties of the initiating photons will be modified during amplification. This effect was predicted theoretically by Lewenstain [29] and investigated experimentally using the SRS signal by Walmsley et al. [30] and the ASE signal by Radziewicz et al. [31].

Typical examples of the ASE and SRS spectra with periodic structure for low- and high-gain media are exhibited in Figs. 7a and 7b. The spectra were measured as a function of time, after one pass through the cell. The average laser power was 7 kW. As can be seen in Fig. 7a, the mode structure is very well resolved in the case of low gain in the system. When the gain increases the mode structure starts to be washed out (laser pump power 9 kW). Of course, the experimental curve still has some statistical variations due to the small ensemble used and the poor spectral quality of the exciting beam. We remember from the theoretical considerations that above the 7 kW pump power level, saturation takes place.

In order to find how the background laser emission influences the mode structure of the generated spectrum we cleaned the output laser beam using a preliminary monochromator. A Jobin-Yvon diffraction grating of 1800 l/mm was used to increase the spectral purity of the beam. Such spectral purity is important in preventing undesired seeding of the ASE and SRS signals. The example of an ASE spectrum obtained in this way is shown in Fig. 8 which shows that the temporal evolution

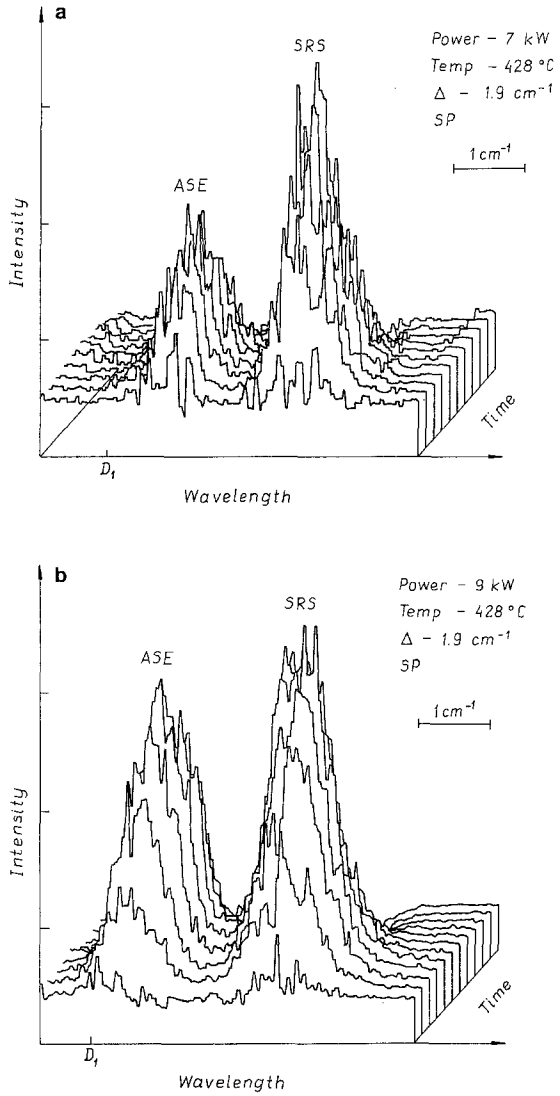

Fig. 7a, b. Time evolution of ASE and SRS spectra. Excited laser power: (**a**) 7 kW, (**b**) 9 kW, laser detuning $\Delta = 1.9\ \mathrm{cm}^{-1}$

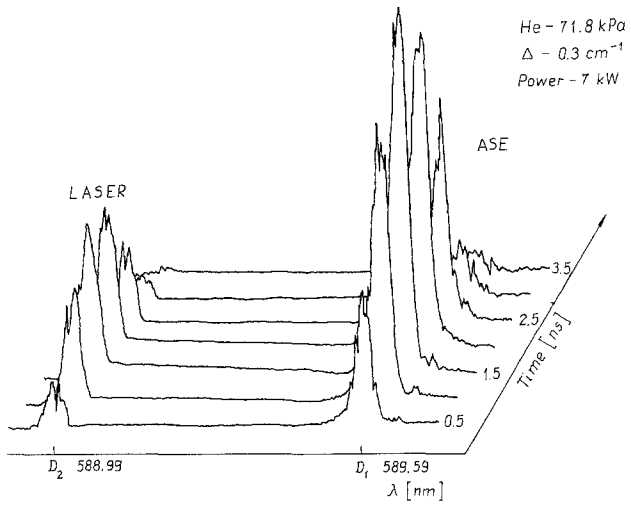

Fig. 8. Time evolution of ASE power spectrum excited by monochromatic illumination. Laser detuning $0.3\ \mathrm{cm}^{-1}$

of the ASE power spectrum resulting from averaging of 5 shots per point is consistently regular. In the case of low laser power and small detuning the Raman component is suppressed by the ASE one, since the fluorescence component grows quickly enough and much of the pump light can be converted to fluorescence before the Raman component becomes stimulated. Figures 9 and 10 show the relative intensity, the line width (HWHM) of the ASE and the pump laser intensity as a function of time in the case when only ASE is generated. These measurements demonstrate that the bandwidth of the ASE radiation first increases with time, beginning with a small fluctuating value, then attains its maximum and thereafter decreases with time.

Figures 9 and 10 show how the ASE bandwidth changes with time at small (34.6 kPa) and high (83.8 kPa) buffer gas pressure. For high buffer-gas pressure the change in the width in time is small and the ASE signal is broader than in the case of small pressure. This behavior can be explained as a contribution of pressure broadening to the line profile. The width of the ASE signal is about $1\ \mathrm{cm}^{-1}$ at the maximum and narrows down to about $0.5\ \mathrm{cm}^{-1}$ at the end of the pulse. Intuitively, such a change in the ASE line shape with time can be explained by taking into account that during the transient build-up of the modes from spontaneous noise, mode competition is not important since initially the gain is unsaturated. Many modes can then be initially established. In the ASE or Stokes spectrum the dominant frequency component appears near the line center as the signal progresses in time, where the gain is bigger. All other frequency components are in a spectral region with less gain. Such an effect produces a gain-narrowed line in the tail of the pulse. Such a narrowing in the one-photon amplifier was predicted by (3).

Figure 11 indicates how the Raman line width and intensity change in time for different helium pressures and large detuning. The biggest Raman intensity was obtained for the lower gas pressure. For this pressure the SRS line width is also narrowed. As already known, for large detuning and low buffer-gas pressure the ASE signal is suppressed, and in this case the gain of the SRS signal increases. In fact, one may expect that for large gain the line width will be reduced in accordance with (4). A pressure broadening effect should also be included in the line profile. One should take into account that with the pump radiation in the form of pulse, the central frequency of the Stokes wave would be swept during the pulse. There would also be pulse reshaping of the Stokes wave during its propagation, due to the spread of frequencies implied by its pulse shape experiencing different gains. In addition, the ASE transition can drastically shorten the effective lifetime of the Raman level, thus resulting in broadening of the Raman transition. These effects are therefore sources of line broadening. The resulting line profile, as mentioned above, becomes the convolution of the line profiles produced by each individual process.

Figure 11 shows that the spectral line width of the generated Stokes radiation is in the range 0.2–$1.2\ \mathrm{cm}^{-1}$, and within this range the line width is observed to in-

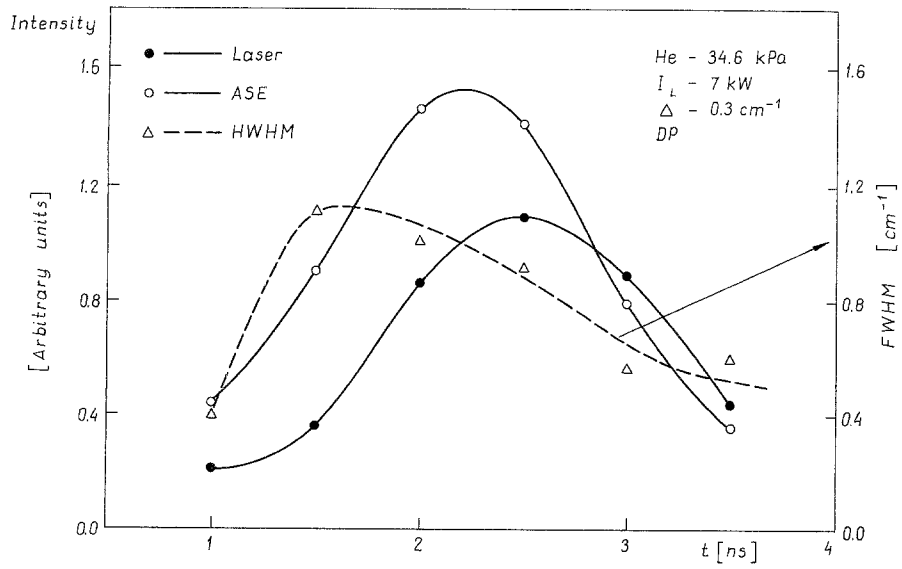

Fig. 9. Relative intensity of the ASE and the laser pulse and the line width (FWHM full width at half maximum) values as a function of time. (Buffer gas pressure 34.6 kPa)

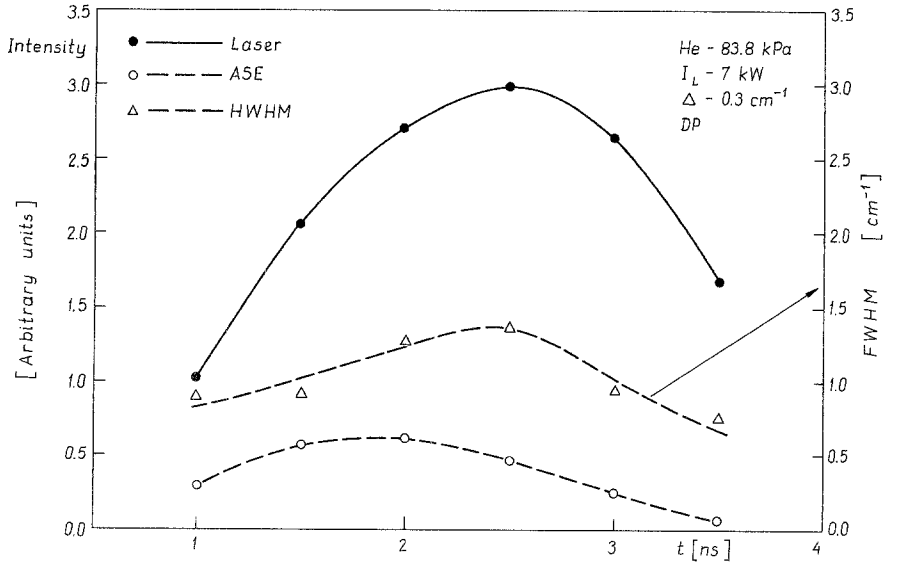

Fig. 10. Relative intensity of the ASE and the laser pulse and the line width values as a function of time. (Buffer gas pressure 83.8 kPa)

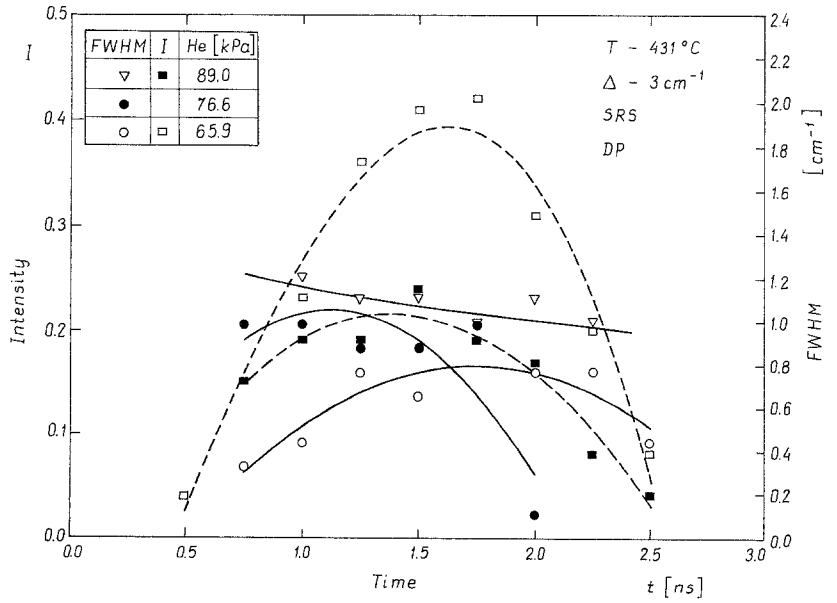

Fig. 11. Growth of the Raman intensity *(dashed line)* and line width *(solid line)* with time for different buffer gas pressures

crease as the buffer gas pressure is raised from 65.9 kPa to 89.0 kPa. Figures 9–11 indicate that the change in the line profile in time for SRS is similar to that of ASE. This is not surprising since, as mentioned earlier, the Raman emission is ASE-like in our case. In the homogeneously broaded amplifier the gain-narrowed process takes place, as follows from (3) and (4) for both types of amplifiers.

4 Conclusion

A detailed study of the spectral and temporal characteristics of collision-aided stimulated processes in sodium vapor in the presence of helium is presented. It was found that ASE and SRS are only present during the laser pulse.

We showed that the ASE signal appears first. This type of behavior is confirmed by the theoretical calculations of Herman et al. [26]. It is further shown how the variation in the pressures of the sodium vapor and buffer gas and detuning influence the time evolution of the ASE signal and Raman emission.

The spectral line widths of these signals change in time. Initially, the fluorescence and Raman radiation are small narrow fluctuating lines. Then their line widths reach the maximum value and thereafter decrease with time. The change in the line profile with time for ASE and SRS is thus similar.

Both line widths change in time from $0.2\,cm^{-1}$ to a maximum of $1.5\,cm^{-1}$ during the time interval the signals are generated. At the end, the line widths are of the order of $0.5\,cm^{-1}$. This agrees with the results of most previous time-independent measurements where the Stokes line width typically varies from 0.3 to $1.0\,cm^{-1}$ when using $0.1\,cm^{-1}$ line width pump sources [31].

Acknowledgements. The authors wish to thank Dr. W. Miklaszewski for helpful discussion and R. Mirkiewicz for invaluable optomechanical design skills.

References

1. J.E. Golub, T.W. Mossberg: Phys. Rev. Lett. **59**, 2149 (1987)
2. Y. Shevy, M. Rosenbluh: J. Opt. Soc. Am. B **5**, 116 (1988)
3. S.N. Atutov, A.I. Plekhanov, A.M. Shalagin: Opt. Spectrosc. SSSR **56**, 215 (1984)
4. J. Czub, J. Fiutak, W. Miklaszewski: Z. Phys. D **3**, 23 (1986)
5. Z. Konefal, M. Ignaciuk: Appl. Phys. B **51**, 258 (1990)
6. A.A. Dabagyan, M.E. Movsessyan, T.H. Ovakimyan, S.V. Shmavonyan: Zh. Eksp. Teor. Fiz. **85**, 1203 (1983)
7. A.A. Dabagyan, M.E. Movsessyan, T.H. Ovakimyan, S.V. Shmavonyan: Izv. Akad. Nauk SSSR Fiz. **47**, 1609 (1983)
8. M. Jyumoii, T. Kobayasi, H. Inaba: Kvant. Elektron. SSSR **3**, 790 (1975)
9. J.J. Wynne, P.P. Sorokin: J. Phys. B **8**, L37 (1975)
10. J.L. Carlsten, A. Szoke, M.G. Raymer: Phys. Rev. A **15**, 1079 (1977)
11. M.G. Raymer, I.A. Walmsley, J. Mostowski, B. Sobolewska: Phys. Rev. A **32**, 332 (1985)
12. R.C. Swason, P.R. Battle, J.L. Carlsten: Phys. Rev. A **45**, 1932 (1992)
13. Z. Konefal, M. Ignaciuk: Z. Phys. D **27**, 49 (1993)
14. D.C. Hanna, M.A. Yuratich, D. Cotter: *Nonlinear Optics of Free Atoms and Moleculs,* Springer Opt. Sci., Vol. 17 (Springer, Berlin, Heidelberg 1979)
15. A.A. Radzig, B.M. Smirnov: *Reference Data on Atoms, Molecules and Ions,* Springer Ser. Chem. Phys., Vol. 31 (Springer, Berlin, Heidelberg 1985)
16. D. Cotter, D.C. Hanna, R. Wyatt: Appl. Phys. **8**, 333 (1975)
17. W. Demtröder: *Laser Spectroscopy* (Springer, Berlin, Heidelberg 1979)
18. R.B. Miles, S.E. Harris: IEEE J. QE-**9**, 471 (1973)
19. D.R. Rockwell, H.W. Bruesselbach: In *Physic of New Laser Sources,* ed. by Abrham, NATO, ASI Series B: Physics, Vol. 132
20. R.W. Dreyfus, R.T. Hodgson: Phys. Rev. A **9**, 2635 (1974)
21. A. Penzkofer, A. Laubereau, W. Kaiser: Prog. Quant. Electron. **6**, 55 (1979)
22. L.W. Casperson, A. Yariv: IEEE J. QE-**8**, 80 (1972)
23. M.G. Raymer, J. Mostowski: Phys. Rev. A **24**, 1980 (1981)
24. B.J. Herman, J.H. Eberly, M.G. Raymer: Phys. Rev. A **39**, 3447 (1989)
25. D.C. MacPherson, R.C. Swanson, J.L. Carlsten: Phys. Rev. A **39**, 3487 (1989)
26. W.G. Raymer, Z.W. Li, I.A. Walmsley: Phys. Rev. Lett. **15**, 1586 (1989)
27. D.C. MacPherson, R.C. Swanson, J.L. Carlsten: Phys. Rev. Lett. **61**, 66 (1988)
28. Mao-hong Lu, Yu-mei Liu: Appl. Phys. B **54**, 288 (1992)
29. M. Lewenstain: Z. Phys. B **56**, 69 (1984)
30. I.A. Walmsley, M.G. Raymer, T. Sizer II, I.N. Duling III, J.D. Kafka: Opt. Commun. **53**, 137 (1985)
31. C. Radzewicz, Z.W. Li, W.G. Raymer: Phys. Rev. A **37**, 2039 (1988)
32. J.C. White: In *Tunable Lasers,* 2nd edn., ed. by L.F. Mollenauer, J.C. White, C.R. Pollack, Topics Appl. Phys., Vol. 59 (Springer, Berlin, Heidelberg 1992) Chap. 4